Est. 1984

ORIENTAL JOURNAL OF CHEMISTRY

An International Open Access, Peer Reviewed Research Journal

www.orientjchem.org

ISSN: 0970-020 X
CODEN: OJCHEG
2023, Vol. 39, No.(6):
Pg. 1556-1570

Synthesis, Characterization, and Computational Study of Novel 2-Phenoxyethyl Xanthate Ligand and Complexes with some Transitions Metals

MOHAMMED MAHMOUD MOLLA-BABAKER[1]*, MAHER KHALID[1], and SAAD. E. AL-MUKHTAR[2]

[1]Department of Chemistry, Faculty of Science, University of Zakho, Zakho, Kurdistan Region, Iraq.
[2]Department of Chemistry, College of science, University of Mosul, Iraq.
*Corresponding author E-mail: mohammed.babaker@uoz.edu.krd

http://dx.doi.org/10.13005/ojc/390616

(Received: August 04, 2023; Accepted: November 18, 2023)

ABSTRACT

The research focuses on the synthesis and characterization of a novel xanthate ligand and their complexes with the formula $[M(PhOEtXant)_2]$, where M represents as Mn(II), Fe(II), Co(II), Ni(II), Cu(II), and Zn(II), and PhOEtXant stands for 2-Phenoxyethylxanthate. The antioxidant activities of these complexes will be evaluated by comparing them with standard natural antioxidants and ascorbic acid using the (DPPH) assay. The synthesized complexes were thoroughly characterized based on their physical properties using various spectral methods, like XRD, FTIR, NMR, AA, UV-Visible, magnetic properties, and conductivity measurements. The complexes are nonelectrolytes, according to molar conductance measurements. Infrared spectra revealed that the ligand acts as a neutral bidentate moiety in all the compounds. Electronic spectra and effective magnetic moments suggested that the compounds exhibit a tetrahedral shape, which is supported by the experimental data. For further insights into the geometry, bond length, bond angle, electronic characteristics, and thermodynamic factors of the synthesized compounds, a density functional theory (DFT) approach with the basis set GGA-PBE was employed for optimization. The antioxidant evaluation using the DPPH assay demonstrated that all the complexes displayed significant radical scavenging activity when compared to the standard ascorbic acid. Remarkably, the Cu, Zn, Ni, and Mn complexes showed superior radical scavenging activities compared to the other complexes and the standard ascorbic acid. Overall, this research highlights the promising potential of the synthesized complexes as effective antioxidants, showcasing their value for further exploration in various applications related to antioxidant research and potentially in therapeutic contexts. The comprehensive characterization using a range of spectroscopic and computational techniques provides valuable insights into their structure and properties, supporting their potential applications in diverse fields of chemistry.

Keywords: Xanthate Salt, Coordination of Xanthate, Tetra-coordinate complexes & complexes of Xanthate.

INTRODUCTION

Alkyldithiocarbonates ($ROCS_2$), also known as xanthate, are a significant kind of 1, 1 dithiolate ligands that have been heavily considered[1]. Indeed, these compounds possess the unique ability to form insoluble complexes in water with various coordination metals. Consequently, they are frequently utilized for the purpose of separating and quantitatively measuring transition metal cations.[2] Coordination compounds featuring bidentate dithio ligands, which can simultaneously bind to a central metal ion, forming a chelate ring. The chelation results in a four-membered metallacycle or metallocycle, where the metal ion is coordinated by two sulfur atoms in a cyclic arrangement. These compounds showcase remarkable properties and structures, and in some cases, they display distinctive and unparalleled characteristics. Xanthates ($RCOS_2$-) are among the most extensively studied sulfur-containing ligands, and their interaction with various metal ions has been a subject of investigation for many years[3,4]. Absolutely correct! Xanthates are generated by the reaction of a metal alkoxide with carbon disulfide. This versatile process enables the xanthation of a wide array of alcohols, making it a valuable method for creating various xanthate compounds with different chemical properties and applications[5]. Xanthates are indeed a kind of organic compounds with a diverse range of uses, which has piqued the interest of chemists. Their significance stems from their widespread use in industry, analytical chemistry, and coordination chemistry. Due to their versatile properties and varied applications, xanthates have become a subject of considerable interest and exploration for investigator in the discipline of chemistry[6]. You are absolutely correct. Molecular geometry optimization is a crucial and fundamental stage in a computational chemistry investigation. The accuracy and reliability of computed parameters, such as energies, vibrational frequencies, and electronic properties, heavily depend on the optimized molecular geometry. In the molecular geometry optimization process, the positions of the atoms in the molecule are adjusted iteratively to find the arrangement that corresponds to the minimum energy or most stable structure. This is achieved by solving the equations of motion for the atoms within the framework of quantum mechanics or molecular mechanics, depending on basis set of theory achieved. The initial geometry predictions play an important function in determining the convergence and success of the optimization process. Various shapes and arrangements are often employed as initial guesses for the positions of atoms in the molecule, including experimental geometries, random geometries, or geometries from similar molecules. The choice of the initial geometry can influence the efficiency of the optimization and whether it converges to the global minimum or a local minimum on the potential energy surface. The optimized molecular geometry serves as the starting point for subsequent calculations, such as electronic structure calculations, molecular dynamics simulations, or property predictions. Hence, it is essential to ensure that the molecular geometry optimization is well-converged and reliable to obtain accurate and meaningful results in computational chemistry investigations[7].

DFT is a popular and efficient method extensively employed to calculate the electronic properties of large systems. It is expected to continue being the preferred approach for obtaining precise geometries in the foreseeable future[8]. We present the preparation and physical characterization of potassium 2-phenoxyethyl xanthate ligands and their metal complexes with divalent transition metal ions (MnII to ZnII), as well as the computation of structures and electronic properties using the DFT method.

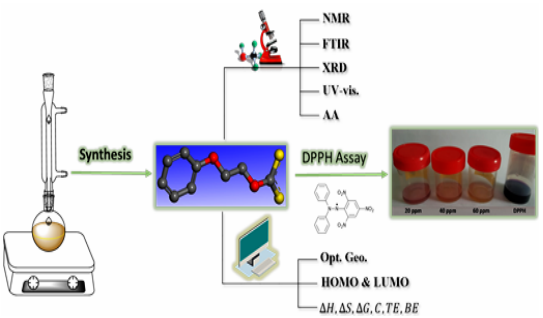

Fig. 1. Graphical Abstract

Experimental and Methodology

The research employed chemicals, reagents, and solvents of analytical grade. Carbon disulfide and 2-Phenoxyethanol were bought from Aldrich company, metal chloride salts were obtained from Alpha company. Ethanol, dimethylformamide (DMF), and diethyl ether were purchased from Scharlau Company. The NMR analysis, including ^{1}H-NMR and ^{13}C-NMR, as well as Dept-135 spectra, were conducted using Bruker 500 and 300 MHz Ultrashield instruments. Deuterated

dimethylsulfoxide (DMSO) was used as the solvent. XRD crystallography diffraction patterns were characterized at 25°C with a range of 2θ=(10°-80°) using Cu radiation (α=1.5405 Å). The potassium bromide disc was used to generate FT-IR spectra on a Perkin-Elmer 1710 spectrophotometer from 350 cm^{-1} to 4000 cm^{-1}. Electronic spectra were measured using a Unicam HEλIOS UV-Vis. 2000 spectrophotometer instrument in DMF solvent with a concentration of 10^{-3} M at 25°C, utilizing 1 cm quartz cells. Magnetic measurements were made in the solid state at 25°C using the Gouy method and a Sherwood scientific magnetic susceptibility balance. A thermal electro-melting point apparatus 9300 was used to measure the melting points or decomposition temperatures of ligands and their complexes. Complex conductivity measurements were performed at 10^{-3}M concentration in DMF solvent at 25°C using an EC214 conductivity meter. Finally, the concentration of metal was determined by atomic absorption AA670. The utilization of various techniques and instruments provided a comprehensive characterization of the prepared ligand and complexes, enabling a detailed analysis of their properties and potential applications.

Synthesis of Potassium 2-phenoxy ethyl xanthate Ligand

2.80 gm (0.05 mol) of potassium hydroxide (KOH) was added to 6.90 g (0.05 mol) of 2-Phenoxyethanol in the synthesis process, and the mixture was refluxed for 1 hour. After refluxing, the mixture was allowed to cool in an ice bath for 30 min while still in the ice bath, and 3.80 g (0.05 mol) of carbon disulfide (CS_2) was added drop-wise with continuous stirring (Fig. 2). TLC was used to track the course of the reaction until it was completed. The reaction produced a yellow precipitate. This precipitate was then washed twice with 50 mL of diethyl ether to purify it. Afterward, the product was recrystallized with ethanol and then dried under vacuum conditions. Overall, this synthesis procedure aimed to produce a specific compound through the reaction of potassium hydroxide with 2-Phenoxyethanol and subsequent addition of carbon disulfide. The process involved refluxing, cooling, and careful monitoring of the reaction progress using TLC to ensure the successful formation of the desired product. The final product was obtained by purification through washing, recrystallization, and drying[9].

Preparation of the tetra coordinated complexes [M(2-Phenoxyethylxanthate)2]

An acidic ethanol solution of $MnCl_2.4H_2O$ (1.98 g, 0.01 mol), or $FeCl_2.4H_2O$ (1.98 g, 0.01 mol), or $CoCl_2.6H_2O$ (2.38 g,0.01 mol), or $NiCl_2.6H_2O$ (2.38 g, 0.01 mol) or $CuSO_4$ (1.60 g,0.01 mol) or $ZnCl_2$ (1.36 g, 0.01 mol) was added drop by drop to an ethanolic solution of potassium 2-Phenoxyethylxanthate (5.04 g,0.02 mol) with stirring for 30 until complete precipitation of the desired metal xanthate complexes. After the precipitation, the resulting precipitate was filtered out and washed with ethanol to remove any impurities. Then, it was rinsed with diethyl ether for further purification. Finally, the washed precipitate was vacuum dried to obtain the final product in its solid form.

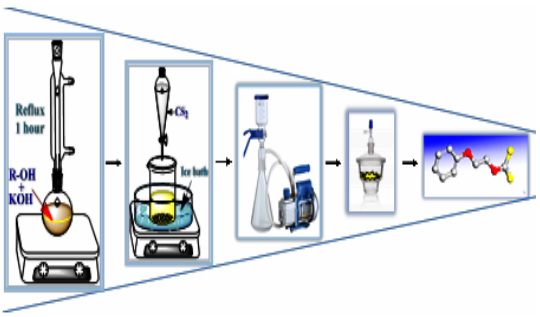

Fig. 2. Graphical procedure for synthesis of potassium 2-phenoxy ethyl xanthate

Computational study

The theoretical calculations for the ligand and their complexes were carried out using DFT method with the Material Studio program. The DFT calculations were carried out with the Dmol3 module, utilizing (GGA) and (PBE) as the basis set. The DFT method is widely used in computational chemistry to study the electronic structure, geometry, and features of molecules and materials. It provides valuable insights into molecular geometries, bond lengths, bond angles, electronic characteristics, and thermodynamic parameters. The optimization of the geometry involves finding the most stable configuration of atoms in the molecule or complex by minimizing the energy. The DFT calculations with GGA and PBE basis set allow for accurate and reliable optimization of the molecular structures. By performing DFT calculations, researchers can gain a deeper understanding of the synthesized ligand and their metal complexes, which can aid in elucidating their properties and potential applications.

The results obtained from these quantum chemical calculations complement the experimental data and contribute to a comprehensive characterization of the synthesized compounds[10].

RESULTS AND DISCUSSIONS

The 1, 1-dithiolate ligand was synthesized by reacting 2-phenoxyethanol with carbon disulfide in a basic medium using potassium hydroxide. The complexes of metal were prepared by reacting the metal chloride or sulfate salts, with the molar ratio of 1:2 ligand, as depicted in Scheme 1. The conductivity values of the prepared complexes were reported in dimethylformamide (DMF) solution, and they were found to be in the range (14.20-41.9) $\Omega^{-1}.cm^2.mol^{-1}$. These conductivity values indicate that the prepared complexes behave as non-electrolytes. Various physical properties of the prepared compounds have been characterized and described in Table 1. These physical features likely include properties such as melting points, color, metal content and other relevant characteristics that can help in understanding the nature of the synthesized compounds.

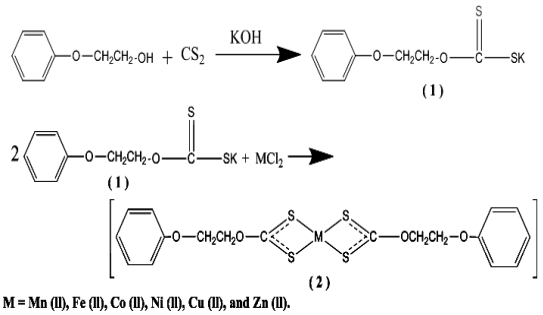

Scheme 1. Preparation of Ligand and Complexes of Potassium 2-Phenoxyethyl Xanthate

Table 1: Some of the produced complexes' physicochemical properties

No.	Compounds	Colors	m.p.°C	Molar conductivity $\Omega^{-1}.cm^2.mol^{-1}$	M%(Cal., Found)	Yield %
L	K (2-PhOEtXant)	Yellow	> 285	----	----	82.67
1	[Mn(2-PhOEtXant)$_2$]	Grey	295	18.3	11.41 (11.13)	24.92
2	[Fe(2-PhOEtXant)$_2$]	Brown	270*	19.7	11.58 (11.24)	78.35
3	[Co(2-PhOEtXant)$_2$]	Green	183*	26.3	12.14 (11.85)	64.05
4	[Ni(2-PhOEtXant)$_2$]	Yellow	175	14.2	12.09 (11.98)	96.23
5	[Cu(2-PhOEtXant)$_2$]	Light Green	229	26	12.97 (12.70)	95.89
6	[Zn(2-PhOEtXant)$_2$]	White	237*	41.9	13.01 (12.98)	71.14

*Decomposition

Nuclear Magnetic Resonance (NMR) studies

The NMR technique (at 500 MHz and 300 MHz) was used to identify the structure of synthesized compounds. The chemical shift δ in ppm (^{1}H-NMR-500MHz; DMSO) for the ligand Potassium 2-Phenoxyethylxanthate showed the following chemical shifts δ=7.28 (t, *J*=7.7 Hz, 2H, Ar-H),δ=6.93 (dd, *J*=7.8 Hz, 3H, Ar-H), δ=6.91, δ=4.52 (t, *J*=4.9Hz, 2H, CH_2), δ=4.17 (t, *J*=4.9 Hz, 2H, CH_2) as shown in (Figs. 3 & 4). The chemical shift δ of ^{13}C NMR (101 MHz, DMSO) δ 66.42, 69.36, 114.80, 120.89, 121.00, 129.99, 158.84 and the strong signal at 40 belongs to the DMSO solvent, furthermore precision, study the DEPT-135 show three signals on positive side which is for (CH-Ar) with two signals in negative side for 2(CH_2) and disappearance signal at 158.84 in positive and negative sides of DEPT-135 which confirms the signal belongs to the thionyl (C=S) as shown in (Figures 5 & 6).

The chemical shift δ (^{1}H-NMR-300MHz; DMSO) for [Zn(2-PhOEtXant)$_2$] δ=7.30 (dd, *J*=7.2 Hz, 4H, Ar-H), δ=6.95 (d, *J*=7.4 Hz, 4H, Ar-H),δ= 6.92 (m, *J*=7.3 Hz, 2H, Ar-H), δ=4.89 (t, *J*=5.5 Hz, 4H, 2CH_2), δ=3.99 (t, *J*=5.0 Hz, 4H, 2CH_2) as represent in (Fig. 7). ^{13}C-NMR (76 MHz, DMSO) δ 60.06 & 69.79 for C of 2CH_2 and δ 114.88, 120.89, 129.95, 159.13 for Ar-C and 215 refer to C=S as shown in (Figure 8).

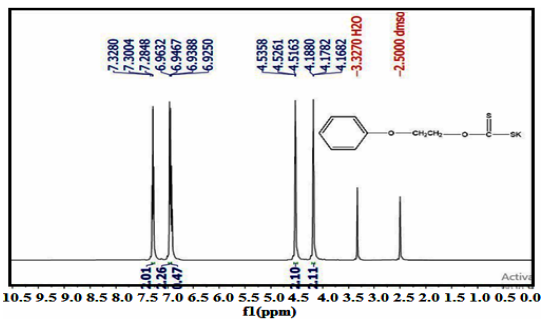

Fig. 3. ^{1}H-NMR of Potassium 2-phenoxyethyl xanthate K (2-PhOEtXant)

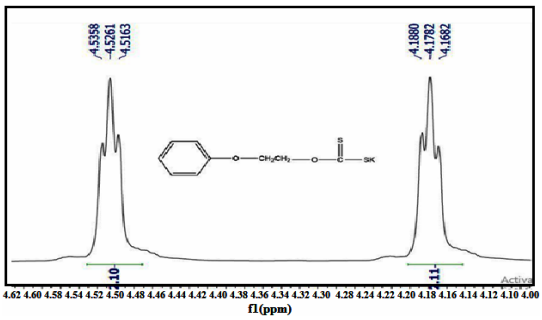

Fig. 4. Expansion ^{1}H-NMR of Potassium 2-phenoxyethyl xanthate K (2-PhOEtXant)

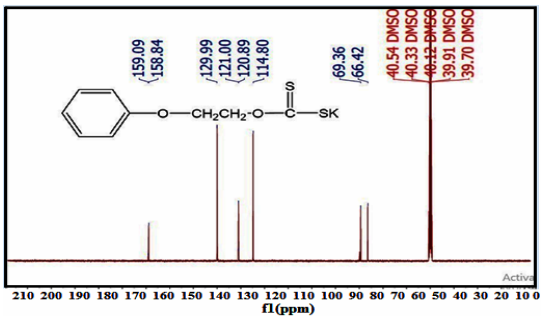

Fig. 5. ^{13}C-NMR of Potassium 2-phenoxyethyl xanthate K (2-PhOEtXant)

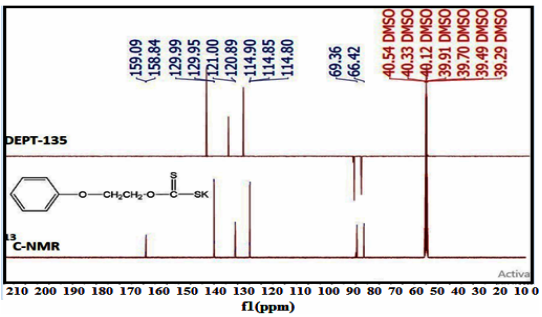

Fig. 6. ^{13}C-NMR & DEPT-135 of Potassium 2-phenoxyethyl xanthate K (2-PhOEtXant)

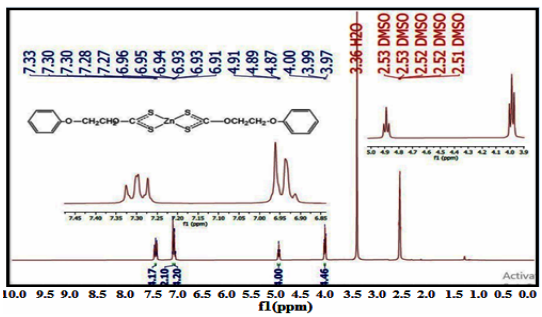

Fig. 7. ^{1}H-NMR of Zinc (II) bis(2-phenoxyethyl xanthato) [Zn (2-PhOEtXant)2]

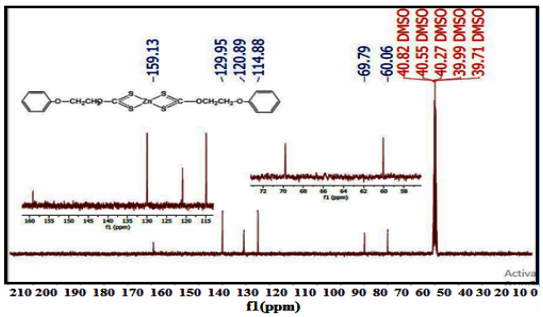

Fig. 8. ^{13}C-NMR of Zinc (II) bis(2-phenoxyethyl xanthato) [Zn(2-PhOEtXant)2]

Infra-red spectral studies

Table 2 presents the most notable FTIR bands found for the ligand (2-PhoEtXant) K and their metal complexes. The chart of ligand observe the band at 1139 cm^{-1} refer to the (C-O-C) vibrations. However, upon complexation, this band shifts to higher frequencies, ranging from (1199–1242) cm^{-1}. Similarly, the band at 1095 cm^{-1} in the ligand spectrum corresponds to the (C-S) vibrations. In the metal complexes, this band transitions to lower frequencies, ranging from 1010 to 1076 cm^{-1}. The shift to lower frequencies indicates an interchange in the bonding environment of the sulfur atoms in the ligand upon coordination with the ions of metal. These shifts in the FTIR bands compared to the ligand's spectrum indicate that the xanthate ligand coordinates with the metal ions through its sulfur atoms, forming metal-sulfur bonds. This coordination behavior is depicted in (Fig. 9). Furthermore, the presence of only one C-S band in the FTIR spectra supports the notion of a symmetrical bidentate binding of the dithiocarbonate molecule to the metal ions. This designates that the ligand forms stable complexes with the ions of metal by chelating through its two sulfur atoms, creating a symmetrical four-membered chelate ring with the metal ion[11,12].

The appearance of the ν(M-S) band in the IR spectra in the range of (354-393) cm^{-1} with medium to strong intensity is indeed a significant

observation and provides compelling verification for the formation of metal xanthate complexes. The chelation of the sulfur atoms to the metal ions leads to the creation of stable complexes. The electron-donating nature of the alcohol (2-phenoxyethanol) moiety in the ligand plays a crucial role in facilitating the coordination process. It generates a high electron density around the sulfur atoms, making them more electron-rich and more likely to form bonds with the metal ions[13]. There is another stretching frequency band appeared in the area 2933 cm^{-1} which attributed to C-H bond of the ligand, in which shifted to the range (2924–2962) cm^{-1} in all complexes.

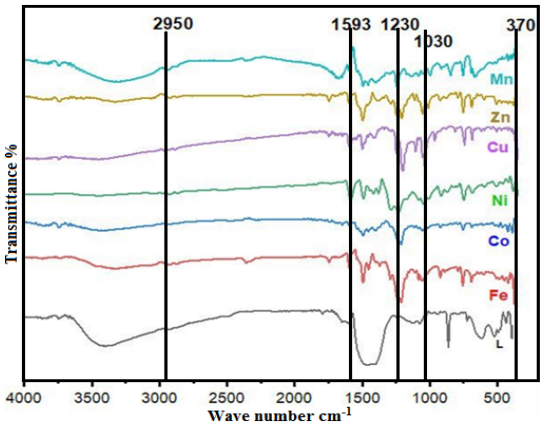

Fig. 9. FTIR Spectra of synthesized compounds

Table 2: The characteristic absorption bands of the FT-IR of the ligand's most significant bonds and their complexes

No	Compounds	υC-H sp^3	υC-H sp^2	υC-O-C	υC-S	υM-S
L	K (2-PhOEtXant)	2933	3043	1139	1095	---
1	[Mn(2-PhOEtXant)$_2$]	2920	3025	1242	1076	393
2	[Fe(2-PhOEtXant)$_2$]	2924	3010	1211	1053	374
3	[Co(2-PhOEtXant)$_2$]	2920	3030	1211	1014	389
4	[Ni(2-PhOEtXant)$_2$]	2924	3059	1230	1045	381
5	[Cu(2-PhOEtXant)$_2$]	2962	3034	1199	1037	354
6	[Zn(2-PhOEtXant)$_2$]	2924	3062	1207	1010	374

XRD Studies & Crystallography

The crystallographic shape of the produced tetra-dentate complexes with potassium 2-phenoxyethyl xanthate bidentate ligand was determined using X-ray Diffraction (XRD) as an analytical technique. In this study, XRD analysis was performed using the X'pert HighScore Plus software to examine the diffraction pattern of each sample. The diffraction pattern obtained from the sample was compared with the diffraction pattern from a reference database using the software. This matching process allows researchers to identify the crystallographic phase of the material. Additionally, Origin Lab software was also utilized to analyze the diffraction pattern from XRD. The XRD measurements were conducted at room temperature with a range of 2θ=(10°-80°) using Cu radiation (α=1.5405 Å). The 2θ value represents the angle of diffraction, and the Cu radiation is used as the X-ray source to interact with the crystal lattice and generate the diffraction pattern.

The crystal pattern of Fe(II), Ni(II) and Zn(II) complexes was found the orthorhombic as matched with the reference code (01-085-0152, 00-024-1838 & 00-026-0572) while the indexing complexes of Co(II) & Cu(II) using X'PertPro soft matched with reference code (01-078-1799 & 00-049-1861) are monoclinic as shown in (Table 6). The measured diffraction pattern of Mn(II) complex was well adjusted to the ICDD reference code 96-410-4900 which is a hexagonal pattern[14,15,16,17,18,19] as illustrated in the Table 3.

Magnetic susceptibility measurements

Table 4 presents the magnetic moments (μ_{eff}) of the complexes designed at room temperature of 25°C. The magnetic moments for the complexes (1- 5) were establish to be in the range of (2.05 - 5.85) B.M. These values indicate a tetrahedral geometry for these complexes.

Table 3: The Crystallographic data according to the XRD information of the compounds

Parameters Crystal System	Mn(II) Hexagonal	Fe(II) Orthorhombic	Co(II) Monoclinic	Ni(II) Orthorhombic	Cu(II) Monoclinic	Zn(II) Orthorhombic
a(A°)	4.8330	5.0952	10.0220	9.7620	8.7550	7.5040
b(A°)	4.8330	10.6370	7.2170	11.0470	13.9870	6.4740
c(A°)	15.9350	17.8810	24.2240	4.9210	17.7300	6.1850
α°	90.0000	90.0000	90.0000	90.0000	90.0000	90.0000
β°	90.0000	90.0000	98.4200	90.0000	104.1300	90.0000
γ°	120.0000	90.0000	90.0000	90.0000	90.0000	90.0000
Z	1.00	4.00	8.00	2.00	8.00	2.00
Space group	R-3	P212121	C2/c	---	C2/c	Pmn21
V ($A^{\circ 3}$)	322.34	969.11	1733.21	530.68	2105.46	300.47

The effective magnetic moment $\chi(\mu_{eff})$ is a measure of the magnetic behavior of a compound and provides valuable information about the coordination environment and magnetic interactions in the complexes. In this case, the measured magnetic moments in the specified range suggest a tetrahedral geometry. A tetrahedral geometry is characterized by the central metal ion surrounded by four ligands, forming a three-dimensional tetrahedral arrangement[20]. Additionally, the complex of Zn(II) was found to be diamagnetic. Diamagnetic substances do not exhibit any magnetic behavior. This observation indicates that the Zn(II) complex does not possess any unpaired electrons and is therefore diamagnetic.

Analyzing electronic spectra

The UV-Visible spectra of the ligand and its complexes were recorded using a (0.001 M) solution in DMF (Dimethylformamide). The results obtained from the spectra were compiled and presented in Table 4. The spectrum of complex 1 shows absorption bands at (34129 & 31446 cm^{-1}) that are related to charge transfer transitions. Due to the presence of five unpaired electrons in the high spin d5 manganese (II) configuration, the (d-d) electronic transitions are both spin-forbidden and Laporte-forbidden. As a result, absorption intensities in the typical (d-d) absorption band are approximately 100 times lower. As a result, the spectra are not visible in the visible spectrum[21,22].

The UV-Visible spectra of the complex 2 gives a signal at (10928 cm^{-1}), which refer to ($^5E \rightarrow {}^5T_2$) transition in a tetrahedral shape as shown in (Fig. 10)[20]. Further, the complex of Co(II) recoded an absorption bands at (10881 & 16233 cm^{-1}) in UV-Vis spectrum, which were designated to undergo transition of (($^4A_2(F) \rightarrow {}^4T_1(F)$) & $^4A_2(F) \rightarrow {}^4T_1(P)$) and correspondingly in tetrahedral configuration of this complex[23], the absence of ($^4A_2(F) \rightarrow {}^4T_2(F)$), could be attributed to the instrument's sensitivity. Moreover, in a tetrahedral structure, the complex of Ni(II) exhibits two absorption bands at (10952 cm^{-1}) and (15267 cm^{-1}) that were assigned to ($^3T_1(F) \rightarrow {}^3A_2(F)$) and ($^3T_1(F) \rightarrow {}^3T_1(P)$) transitions, respectively.[20] Furthermore, the Cu(II) complex has an absorption band at (11261 cm^{-1}) that corresponds to the ($^2T_2 \rightarrow {}^2E$) transition in a tetrahedral geometry[24]. On the other hand, the complex of Zn(II) metal sense no peak in the visible region because of (d^{10}-system) that signifies that no (d-d) electronic transfer occurred. The prepared complex is diamagnetic which is expected for d^{10} ion. According to effective magnetic moment, these metals do not show (d-d) transition[25,26].

It appears that for all the compounds under study, the UV-Visible spectra show distinct absorption bands at specific wavenumbers. The high-intensity absorption peaks observed in the range of 35587 to 47393 cm^{-1} are attributed to ($\pi \rightarrow \pi^*$) and ($n \rightarrow \pi^*$) intra-ligand transitions. Intra-ligand transitions involve the excitation of electrons within the ligand molecule, specifically between its π orbitals ($\pi \rightarrow \pi^*$) or between non-bonding electron pairs and ϖ orbitals ($n \rightarrow \varpi^*$).

On the other hand, the low-intensity bands observed in the near UV region, ranging from 26315 to 35971 cm^{-1}, are assigned to ligand to metal charge transfer (LMCT) bands transitions. In LMCT transitions, electrons transfer from the ligand orbitals to the metal orbitals, resulting in characteristic absorption bands in the UV-Visible spectrum[27,28].

These spectral features provide valuable information about the electronic structure and bonding interactions within the coordination complexes. The different absorption bands and their corresponding wavenumbers offer insights into the nature of electronic transitions, the coordination environment, and the stability of the complexes. The interpretation of the UV-Visible spectra allows researchers to understand the energy levels of the molecular orbitals and the distribution of electronic states in the coordination complexes. This information is essential for elucidating the properties and potential applications of the compounds in various fields of chemistry and material science.

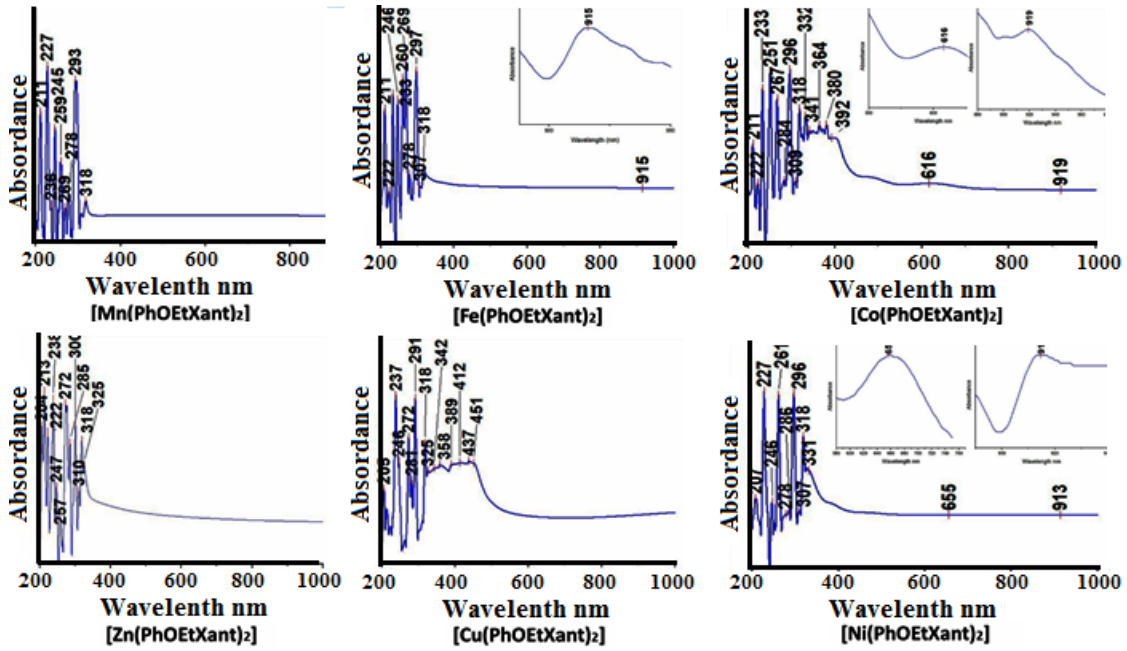

Fig. 10. UV-Visible Spectra of synthesized compounds

Table 4: The electronic spectrum data and effective magnetic moment values of ligands and formed compounds

No	Compounds	U-Vis bands (cm^{-1})	Assignment	μ_{eff} B.M	Proposed Structure
L	K(2-PhOEtXant)	46728, 42372, 39682, 35211	$\pi\rightarrow\pi^*$, $n\rightarrow\pi^*$	----	----
1	[Mn(2-PhOEtXant)$_2$]	47393, 44052, 40816	$\pi\rightarrow\pi^*$, $n\rightarrow\pi^*$	5.85	Tetrahedral
		34129, 31446	C.T		
2	[Fe(2-PhOEtXant)$_2$]	47393, 45045, 40650	$\pi\rightarrow\pi^*$, $n\rightarrow\pi^*$	4.80	Tetrahedral
		35971, 33670, 31446	C.T		
		10928	($^5E\rightarrow{}^5T_2$)		
3	[Co(2-PhOEtXant)$_2$]	45045, 39840, 37453	$\pi\rightarrow\pi^*$, $n\rightarrow\pi^*$	3.82	Tetrahedral
		30120, 27472, 26315	C.T		
		16233, 10881	($^4A_2(F)\rightarrow{}^4T1(P)$)&($^4A_2(F)\rightarrow{}^4T_1(F)$)		
4	[Ni(2-PhOEtXant)$_2$]	44843, 41322, 38022, 36764	$\pi\rightarrow\pi^*$, $n\rightarrow\pi^*$	2.97	Tetrahedral
		31347, 30674, 26385	C.T		
		15267, 10952	($^3T_1(F)\rightarrow{}^3A_2(F)$)&($^3T_1(F)\rightarrow{}^3T_1(P)$)		
5	[Cu(2-PhOEtXant)$_2$]	42194, 40650, 35587	$\pi\rightarrow\pi^*$, $n\rightarrow\pi^*$	2.05	Tetrahedral
		25706, 25271	C.T		
		10261	($^2T_2\rightarrow{}^2E$)		
6	[Zn(2-PhOEtXant)$_2$]	46948, 42016, 38910, 36764	$\pi\rightarrow\pi^*$, $n\rightarrow\pi^*$	Dia	Tetrahedral
		32258, 31446, 30769	C.T		

Antioxidant activity assay using DPPH Method

The method described is a widely used and simple way to screen for antioxidant activity in foods and plant drugs. The antioxidant capacity is evaluated using the DPPH free radical. The ligand, potassium 2-phenoxyethyl xanthate, and its four coordinate complexes are dissolved in dimethyl sulfoxide (DMSO) and then diluted in methanol to obtain a concentration of 200 µg/mL. To assess the antioxidant activity, stock solutions of the ligand and complexes are further diluted to 20, 40, and 60 µg/mL. Each diluted solution is then mixed with 0.5 mL of a freshly prepared methanolic solution of (DPPH) at a concentration of 0.5 mM. The mixtures are incubated at room temperature for 30 minutes. During the incubation period, the compounds in the solutions transfer hydrogen to the DPPH radical, causing a color change from deep violet to pale yellow. This color change indicates the reduction of the DPPH radical, indicating the scavenging of the

radical by the tested compounds. To quantify the DPPH radical scavenging efficiency, the absorbance of the reaction mixtures is measured at 517nm (λ_{max}). The absorbance value is then used to calculate the inhibition percent (IP) of the DPPH radical using the following equation[29,30].

$$IP = \frac{A_C - A_S}{A_C} \times 100$$

Where

A_C=Absorbance of the DPPH radical methanol
A_S=Absorbance of DPPH+sample (tested sample/ standard

The antioxidant capacity of the investigated substances is compared using ascorbic acid as the reference compound. By calculating the inhibition percent (IP), researchers can evaluate the antioxidant activity of the ligand and its four coordinate complexes compared to the reference compound (ascorbic acid). The higher the inhibition percent, the stronger the antioxidant activity of the compounds, indicating their potential as antioxidants in foods and plant drugs[31].

The mean of DPPH scavenging %(IP) of triplicated tasted compounds at various concentrations are listed in Table 4, while the mean of inhibition percent at different concentrations, IC_{50}, Standard Error, Standard deviation, and Coefficient of variation % of IC_{50} was shown in Table 5.

Table 4: Antioxidant Activity of the Ligand and its Metal Complexes

No	Concentration (µg/mL) / Compounds	20	40	60
		Mean of IP (DPPH scavenging %)		
1	(2-PhOEtXant) K	68.07	80.53	88.96
2	[Mn(2-PhOEtXant)$_2$]	52.19	53.75	54.74
3	[Fe(2-PhOEtXant)$_2$]	75.53	81.96	90.00
4	[Co(2-PhOEtXant)$_2$]	66.13	64.75	70.07
5	[Ni(2-PhOEtXant)$_2$]	79.00	78.03	86.54
6	[Cu(2-PhOEtXant)$_2$]	80.55	80.53	98.29
7	[Zn(2-PhOEtXant)$_2$]	90.12	97.94	98.52
8	Ascorbic acid	93.05	93.54	93.88

Table 5: Some analytical parameters and IC_{50}

No	Compounds	Mean of IP at varies conc.	Standard Error	Standard deviation	Coefficient of variation%	IC_{50}
L	(2-PhOEtXant) K	79.1866	1.805	3.1263	3.948	63.88
1	[Mn(2-PhOEtXant)$_2$]	53.56	1.578	2.7331	5.1028	37.82
2	[Fe(2-PhOEtXant)$_2$]	82.4966	1.775	3.0743	3.7265	59.62
3	[Co(2-PhOEtXant)$_2$]	66.9833	1.772	3.0691	4.5818	59.21
4	[Ni(2-PhOEtXant)$_2$]	81.19	1.326	2.2966	2.8286	21.2
5	[Cu(2-PhOEtXant)$_2$]	86.4566	1.197	2.0732	2.3979	15.73
6	[Zn(2-PhOEtXant)$_2$]	95.5526	1.303	2.2568	2.3618	20.08
7	Ascorbic acid	93.4900	1.593	2.7591	2.9512	39.16

The activity of the compounds (L-7) was evaluated based on their inhibitory concentration IC_{50}, which represents the amount of antioxidants required to decrease the initial conc. of DPPH• radicals by 50%. A lower IC_{50} value indicates a higher "antiradical efficiency," meaning that the compound is more effective in scavenging and neutralizing free radicals. Tables 3 and 4 summarize the radical scavenging activity of the compounds. Among the tested compounds, the complexes (Cu, Zn, Ni, and Mn) exhibited better radical scavenging activity with IC_{50} values of 15.73, 20.08, 21.2, and 37.82 µg/mL, respectively, compared to other compounds. Notably, their IC_{50} values were lower than that of ascorbic acid, a well-known antioxidant, which had an IC_{50} value of 39.16 µg/mL. The observed higher radical scavenging activity of these metal complexes (Cu, Zn, Ni, and Mn) suggests that they have potent antioxidant properties.

The generation of free radicals is at the root of many chronic diseases, including cancer, diabetes, and cardiovascular disease[32]. The ability of antioxidants to destroy free radicals is one of their most essential properties. According to scientific evidence, antioxidants reduce the risk of several chronic diseases[33]. In summary, the metal complexes (Cu, Zn, Ni, and Mn) demonstrated superior radical scavenging activity compared to other compounds and even outperformed ascorbic acid, a well-known antioxidant. Their potential as effective antioxidants highlights their significance in mitigating oxidative stress and reducing the risk of chronic diseases.

Computational studies of the complexes

The computational calculations revealed that the metal atoms in the prepared complexes are

coordinated in a tetrahedral geometry, where each metal ion is surrounded by four sulfur atoms from two chelating 2-phenoxyethyldithiocarbonate ligands. This coordination geometry agrees with the predicted structure, as shown in Fig. 11. The calculated bond lengths and bond angles of the complexes are presented in Tables 6 and 7, respectively. These structural parameters provide valuable information about the molecular structure of the complexes. The bond lengths indicate the distances between the metal ion and the coordinating atoms, in this case, the sulfur atoms of the ligands. The bond angles show the angles formed between the metal ion and the ligand atoms. By analyzing these bond lengths and bond angles, researchers gain insights into the spatial arrangement and coordination environment of the metal ion within the complex. The tetrahedral coordination formed by the chelating 2-phenoxyethyldithiocarbonate ligands ensures stability and allows for strong interactions between the metal ion and the ligands. This structural information is essential for understanding the bonding interactions and coordination behaviour of the complexes.

The length of (M-S1, M-S2, M-S3 and M-S4) bonds were found in the range [(1.741-2.323), (1.755-2.322), (1.750-2.324), (1.745-2.323)] respectively, which are acceptance with complexes prepared by Abrahams[14,18-34]. Furthermore, the relatively identical bond length for (C1-S1) and (C1-S2) that observed in the range [(1.680-1.810) & (1.745-1.810)]. Moreover, the length of (C1-O1) bond for all compounds are ranged in (1.346-1.540). In another aspect of the study, the computed bond angles of the complexes were analyzed. The angle bonds of (S1-M-S4 or S1-M-S3), (S2-M-S3 or S2-M-S4), (S1-M-S2) and (S3-M-S4) are found in the range [(90.231-149.162), (89.820-118.779), (69.427-109.471) & (70.286-109.471)][35,36]. As a result, a comparison of the data with literature reports shows that bond distances and bond angles coincide well. The existence of a phenyl ring may be responsible for the little variation in bond lengths and angles.

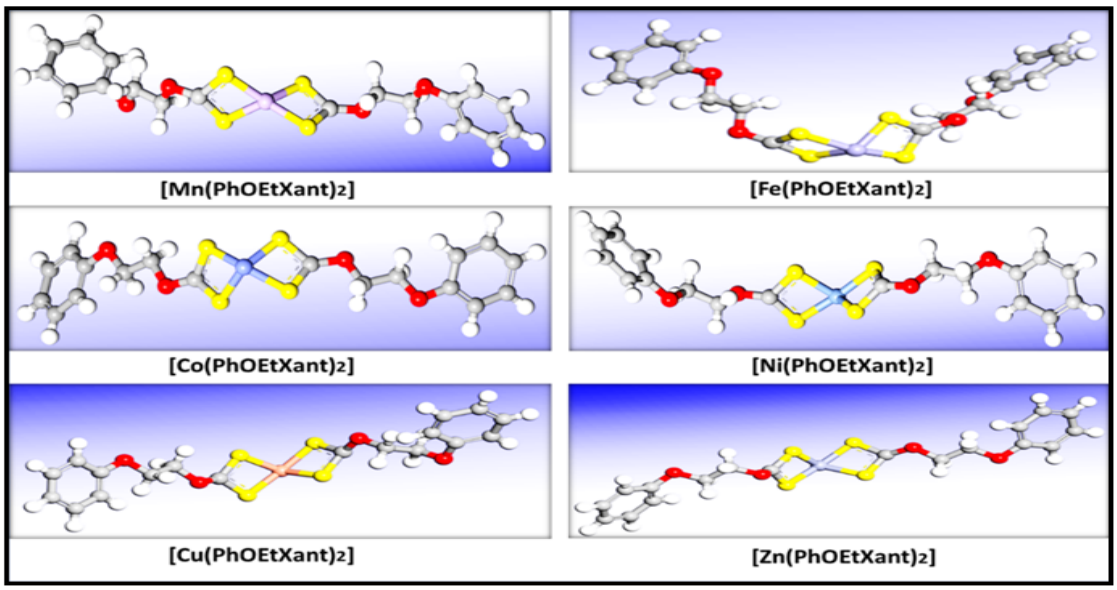

Fig. 11. Optimization the geometry of prepared complexes using DFT Method with Dmol3 using GGA, PBE

Table 6: Geometrical bond length for synthesized ligands and complexes determined by DFT and Dmol3 utilizing GGA and PBE

No.	Compounds	M-S1	M-S2	M-S3	M-S4	C1-S1	C1-S2	C1-O1
L	(2-PhOEtXant) K	---	---	---	---	1.810	1.810	1.540
1	[Mn(2-PhOEtXant)$_2$]	2.310	2.311	2.312	2.312	1.793	1.794	1.507
2	[Fe(2-PhOEtXant)$_2$]	2.323	2.322	2.324	2.323	1.780	1.779	1.510
3	[Co(2-PhOEtXant)$_2$]	2.277	2.274	2.277	2.275	1.780	1.776	1.506
4	[Ni(2-PhOEtXant)$_2$]	2.269	2.269	2.273	2.269	1.785	1.785	1.509
5	[Cu(2-PhOEtXant)$_2$]	2.272	2.271	2.273	2.272	1.785	1.785	1.511
6	[Zn(2-PhOEtXant)$_2$]	1.741	1.755	1.750	1.745	1.680	1.745	1.346

Table 7: Geometrical bond angle for synthesized complexes by DFT, Dmol3 at GGA, PBE level

No	Compounds	S1-M-S4	S2-M-S3	S1-M-S2	S3-M-S4
1	[Mn(2-PhOEtXant)$_2$]	149.162	118.779	72.426	71.571
2	[Fe(2-PhOEtXant)$_2$]	92.838	98.029	69.427	70.286
3	[Co(2-PhOEtXant)$_2$]	90.231	89.820	70.514	70.662
4	[Ni(2-PhOEtXant)$_2$]	103.073	110.103	71.604	71.670
5	[Cu(2-PhOEtXant)$_2$]	97.620	97.760	70.194	70.720
6	[Zn(2-PhOEtXant)$_2$]	109.471	109.471	109.471	109.471

Electronic Properties

The frontier orbitals, specifically the HOMO and LUMO are essential parameters for determining the electrical transport properties and biological activity of molecules. In Fig. 12, the HOMO and LUMO energy levels are depicted, and their energy gap represents the frontier orbital gap. This gap reflects the stability and reactivity of the molecule. A narrow frontier orbital gap suggests strong polarizability, high chemical reactivity, and low kinetic stability, indicating that the molecule is more vulnerable to chemical processes[37,38]. The eigenvalues of the HOMO and LUMO energy levels can also provide insights into the biological activity of the molecule. A molecule with a small energy gap between HOMO and LUMO is more likely to exhibit biological activity[39]. Based on the HOMO and LUMO energy values, various molecular parameters can be calculated. The ionization potential, denoted by Eq. (1), is the least energy required to remove an electron from a gaseous atom or molecule. The electron affinity, as shown in Eq. (2), represents the energy released when adding an electron to a gaseous molecule[40]. The electronegativity of a nucleus, referring to Eq. (3), indicates its tendency to draw electrons towards itself. Chemical hardness, denoted by Eq. (4), is a measure of the resistance of a molecule to undergo electron transfer. A high chemical hardness implies low reactivity[41,42,43]. The electrophilicity, introduced by Parr *et al.,* quantitatively classifies the global electrophilic nature of a compound on a relative scale. It is described by ω, as shown in Eq. (6), which represents the energy lowering due to maximal electron flow between a donor and an acceptor[44]. Overall, these molecular parameters calculated based on the HOMO and LUMO energy values provide valuable insights into the reactivity, stability, and biological activity of the molecules. They are essential in understanding the electronic properties of the molecules and can aid in rationalizing their behavior in various chemical and biological processes. Table 8 displays the electronic structure parameters (EHOMO, ELUMO, EGap), electron affinity (EA), ionization potential (IP), moment of dipole (D), hardness (η), softness (S), absolute electronegativity (ω), chemical potential (μ), and electrophilicity index (χ) determined by DFT, GGA, and PBE techniques.

$$IP = -E_{HOMO} \quad (1)$$

$$EA = -E_{LUMO} \quad (2)$$

$$\chi = -(IP+EA)/2 \quad (3)$$

$$\eta = (IP-EA)/2 \quad (4)$$

$$\mu = (IE+EA)/2 \quad (5)$$

$$\omega = \mu^2/2\eta \quad (6)$$

Thermodynamic Parameters

The study involved calculating thermodynamic parameters using quantum-mechanical methods to establish consistent relations between energetic, structural, and reactivity characteristics of the dithiocarbonate complexes. The thermodynamic characteristics of the ligand and its complexes were calculated using the DFT (Density Functional Theory) approach with Dmol3 code and GGA (Generalized Gradient Approximation) using PBE (Perdew, Burke, and Ernzerhof) functional at a temperature of 298.15 K and a pressure of 1 atm. Table 9 lists the calculated values of these thermodynamic parameters for the ligand and its complexes. Entropy represents the molecular disorder and randomness in the system. Enthalpy is the heat content of the system at constant pressure, while internal energy refers to the total energy of the system. Specific heat capacity indicates the amount of heat needed to raise the temperature of the system by one degree[45].

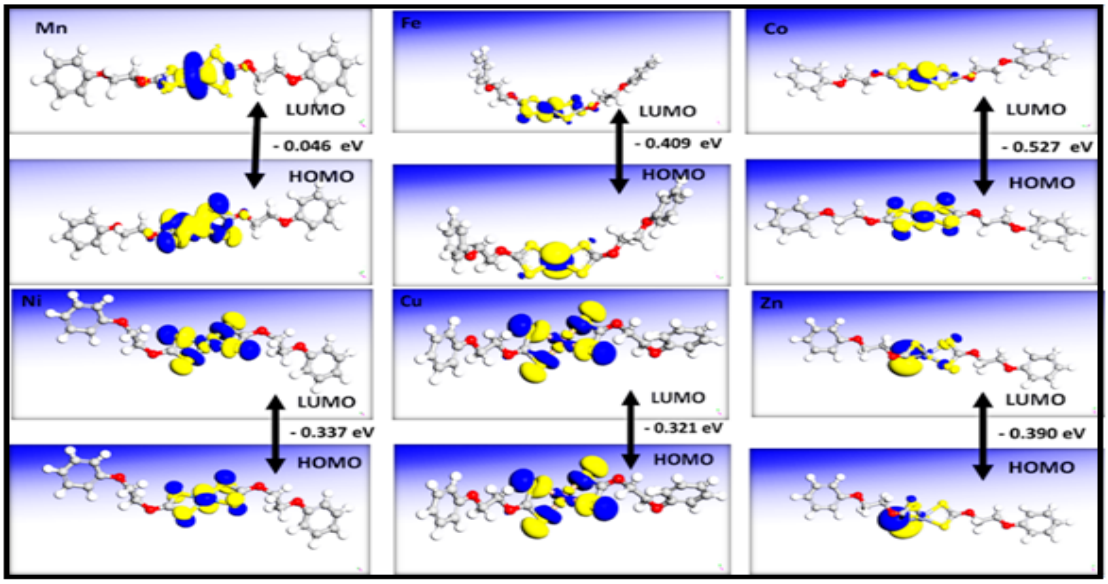

Fig. 12. HOMO, LUMO & gab energy of synthesized complexes using DFT at GGA, PBE level

Table 8: Electronic features calculated of prepared compounds at the level of DFT, Dmol3 using GGA, PBE

Symbol	E_{HOMO}	E_{LOMO}	E_{gap}	(IP)	(EA)	(η)	(S)	(χ)	(μ)	(ω)	(D)
L	-3.988	-2.971	-1.017	3.988	2.971	0.5085	1.9665	-3.4795	3.4795	11.904	11.0430
Mn	-4.775	-4.729	-0.046	4.775	4.729	0.0230	4.3478	-4.7520	4.7520	490.90	1.0533
Fe	-5.096	-4.687	-0.409	5.096	4.687	0.2045	4.8899	-4.8915	4.8915	58.500	3.4338
Co	-4.782	-4.255	-0.527	4.782	4.255	0.2635	3.7950	-4.5185	4.5185	38.741	0.3995
Ni	-4.751	-4.414	-0.337	4.751	4.414	0.1685	5.9347	-4.5825	4.5825	62.312	1.1482
Cu	-4.247	-3.926	-0.321	4.247	3.926	0.1605	6.2305	-4.1000	4.1000	52.367	2.4484
Zn	-4.865	-4.475	-0.390	4.865	4.475	0.1950	5.1282	-4.6700	4.6700	55.920	1.0670

Table 9: Calculated thermodynamical parameters for all complexes with ligand

No	Compounds	Binding energy (kcal/mol)	Total Energy (kcal/mol)	Gibbs free energy (kcal/mol)	Enthalpy (kcal/mol)	Entropy ($calmol^{-1}K^{-1}$)	Specific heat, Cp ($calmol^{-1}K^{-1}$)
L	K (2-PhOEtXant)	-2368.257	-1189104.57	64.489	101.071	122.695	57.645
1	$[Mn(2\text{-}PhOEtXant)_2]$	-5384.309	-2337663.88	165.498	219.370	180.688	95.624
2	$[Fe(2\text{-}PhOEtXant)_2]$	-5398.680	-2408321.63	164.329	221.094	190.391	101.161
3	$[Co(2\text{-}PhOEtXant)_2]$	-5425.135	-2482982.77	163.427	220.618	191.819	101.159
4	$[Ni(2\text{-}PhOEtXant)_2]$	-5429.818	-2561704.45	165.675	218.807	178.206	95.068
5	$[Cu(2\text{-}PhOEtXant)_2]$	-4543.815	-2654884.25	161.185	217.229	187.974	99.409
6	$[Zn(2\text{-}PhOEtXant)_2]$	5271.217	-2731583.28	150.674	200.734	167.904	107.037

CONCLUSION

The synthesis of potassium 2-Phenoxyethylxanthate ligand and its complexes with various transition and non-transition metals was successfully achieved. The complexes were found to exhibit a tetrahedral geometry, which was confirmed by analyzing the spectral data and magnetic susceptibility values. The computational calculations using Dmol3 at the GGA, PBE level provided valuable information on the electronic properties, thermodynamic parameters, bond lengths, and bond angles of all compounds. These calculations were in good agreement with previous publications, validating the accuracy and reliability of the results[46-14].

One of the significant findings of this study is that all the complexes exhibited good radical scavenging activity against DPPH, a stable free

radical widely used for antioxidant testing. Notably, the complexes containing copper (Cu), zinc (Zn), nickel (Ni), and manganese (Mn) demonstrated particularly strong radical scavenging action, surpassing the performance of other compounds as well as ascorbic acid, a well-known antioxidant. This highlights the potential of these complexes as effective antioxidants, which can play a crucial role in mitigating oxidative stress and reducing the risk of chronic diseases.

The motivation behind preparing these complexes was driven by their wide application in various fields, including industrial applications like flotation agents, analytical agents, wastewater treatments, and synthesis of nano-materials. Additionally, their potential in the field of medicine, particularly their biological and cytotoxic activities against human cancer cells, adds further significance to their study.

Furthermore, the characterization and identification of the structures of these complexes contribute to the existing literature and provide valuable data for comparison with the work of other researchers. This not only enhances our understanding of these compounds but also helps to expand the knowledge base in the field of coordination chemistry.

In conclusion, the successful synthesis and characterization of potassium 2-Phenoxyethylxanthate ligand and its metal complexes have led to the identification of their tetrahedral geometry and provided valuable insights into their electronic properties and thermodynamic parameters. The observed good radical scavenging activity of the complexes, especially those containing Cu, Zn, Ni, and Mn, demonstrates their potential as effective antioxidants with various applications in industrial and medical fields. The study also contributes to the existing body of knowledge and opens up avenues for further research and comparison with other published works.

ACKNOWLEDGMENT

This research received no external funding.

Conflict of interest

The author declare that we have no conflict of interest.

REFERENCES

1. S. Sharma.; R. Sachar.; G. D. Bajju and V. Sharma.; "Nickel(II) complexes of m-ethylphenylxanthate with nitrogen donors and their biological screening," *Indian J. Chem. A.*, **2020**, *59*(11), 1618–1626.
2. M. Wang.; Q. Zhang.; W. Hao.; and Z.-X. Sun, "Surface stoichiometry of zinc sulfide and its effect on the adsorption behaviors of xanthate," *Chem. Cent. J.*, **2011**, *5*(1), 1–10, [Online]. Available: https://bmcchem.biomedcentral.com/counter/pdf/10.1186/1752-153X-5-73.pdf.
3. I. Haiduc, "In Comprehensive Coordination Chemistry–II, Meyer, J A and Meyer, T J., Eds., vol. 1." Elsevier., **2004**.
4. A.-C. Larsson and S. Öberg, "Study on potassium iso-propylxanthate and its decomposition products: experimental ^{13}C CP/MAS NMR combined with DFT calculations," *J. Phys. Chem. A.*, **2011**, *115*, (8), 1396–1407.
5. K. Singh.; G. Kour.; R. Sharma.; R. Sachar.; V. K. Gupta.; and R. Kant.; "X-ray crystallography of bis (o-ethylxanthato)-bis (3, 5-dimethylpyridine) nickel (II)," *Eur. Chem. Bull.*, **2022**, *3*(5), 463.
6. S. A. Saah.; M. D. Khan.; J. A. M. Awudza.; N. Revaprasadu.; and P. O'Brien, "A Facile Green Synthesis of Ultranarrow PbS Nanorods," *J. Inorg. Organomet. Polym. Mater.*, **2019**, *29*, 2274–2281.
7. B. Rai, Molecular modeling for the design of novel performance chemicals and materials. CRC Press, **2012**.
8. E. Caldeweyher and J. G. Brandenburg, "Simplified DFT methods for consistent structures and energies of large systems," *J. Phys. Condens. Matter.*, **2018,** *30*(21), 213001.
9. P. D. McNaughter "The effect of alkyl chain length on the structure of lead (II) xanthates and their decomposition to PbS in melt reactions," *Dalt. Trans.*, **2016**, *45*(41), 16345–16353.
10. X. Zhang.; Y. Zhao.; Z. Zhang, and S. Wang, "Investigation of the interaction between xanthate and kaolinite based on experiments, molecular dynamics simulation, and density functional theory," *J. Mol. Liq.*, **2021**, *336*, 116298.

11. S. Andotra.; N. Kalgotra, and S. K. Pandey, "Syntheses, Characterization, Thermal, and Antimicrobial Studies of Lanthanum (III) Tolyl/ Benzyldithiocarbonates," *Bioinorg. Chem. Appl.*, **2014**, 2014.
12. T.-J. Khoo "Synthesis, characterization and biological activity of two Schiff base ligands and their nickel(II), copper(II), zinc(II) and cadmium(II) complexes derived from S-4-picolyldithiocarbazate and X-ray crystal structure of cadmium (II) complex derived fro," Inorganica *Chim. Acta.*, **2014**, *413*, 68–76.
13. H. Rathore.; G. Varshney.; S. Mojumdar.; and M. Saleh, "Synthesis, characterization and fungicidal activity of zinc diethyldithiocarbamate and phosphate," *J. Therm. Anal. Calorim.*, **2007**, *90*(3), 681–686.
14. A. M. Qadir.; S. Kansiz.; N. Dege.; G. M. Rosair.; and I. O. Fritsky, "Crystal structure and DFT study of a zinc xanthate complex," Acta Crystallogr. Sect. E Crystallogr. *Commun.*, **2019**, *75*(11), 1582–1585.
15. A. M. Qadir.; S. Kansiz.; N. Dege.; and E. Saif, "Crystal structure and Hirshfeld surface analysis of bis [(ethoxymethanethioyl) sulfanido](N, N, N, Nλ-tetramethylethane-1, 2-diamine) mercury (II)," Acta Crystallogr. *Sect. E Crystallogr. Commun.*, **2021**, *77*(11), 1126–1129.
16. D. Bibelayi "Hydrogen bonding at C=Se acceptors in selenoureas, selenoamides and selones," Acta Crystallogr. Sect. B *Struct. Sci. Cryst. Eng. Mater.*, **2016,** *72*(3), 317–325.
17. C. M. Read.; M. D. Smith.; and H.-C. Zur Loye, "Single crystal growth and structural characterization of ternary transition-metal uranium oxides: $MnUO_4$, $FeUO_4$, and NiU_2O_6," *Solid state Sci.*, **2014,** *37*, 136–143.
18. B. F. Abrahams.; B. F. Hoskins.; E.R.T. Tiekink, and G. Winter, "Investigation of a new xanthate ligand. The crystal and molecular structures of nickel and cadmium (methoxyethyl) xanthates," *Aust. J. Chem.*, **1988**, *41*(7), 1117–1122.
19. Y. Elerman, "Refinement of the crystal structure of $CoSO_4.6H_2O$," Acta Crystallogr. Sect. C Cryst. *Struct. Commun.*, **1988**, *44*(4), 599–601.
20. D. Nicholls, The chemistry of iron, cobalt and nickel: comprehensive inorganic chemistry, vol. 24. Elsevier, **2013**.
21. H. I. Adel and S. E. Al-mukhtar, "synthesis and characterization of sulfur donor ligand (xanthate) complexe with manganese (ll), iron (ll), cobalt(ll), nikel(ll), copper(ll), and zinc(ll) and thier adduct with nitrogen base ligande," *J. Duhok Univ.*, **2022**, *25*(2), 244–260.
22. S. E. Al-Mukhtar and H. A. Mohammed, "Synthesis and Characterization of Mn(II), Fe(II) and Co(II) Complexes with 4-Hydroxypiperidinedithiocarbamate and their Adducts with Neutral Bases," *J. Sci.*, **2014,** *25*(1), 53–61.
23. K. S. Siddiqi and N. Nishat, "Synthesis and characterization of succinimide and phthalevhde dithiocarbamates and their complexes with some transition metal ions," Synth. *React. Inorg. Met. Chem.*, **2000**, *30*(8), 1505–1518.
24. J. Cookson "Metal-directed assembly of large dinuclear copper(II) dithiocarbamate macrocyclic complexes," *Inorganica Chim. Acta.*, **2010**, *363*(6), 1195–1203.
25. O. O. Wahab.; I. Waziri.; S. O. Oselusi.; S. A. Egieyeh.; G. A. Mala, and H. Nasir, "Zinc (II) complex of (Z)-4-((4-nitrophenyl) amino) pent-3-en-2-one, a potential antimicrobial agent: Synthesis, characterization, electrochemical, antimicrobial, DFT and docking studies," **2022**.
26. I. A Al-Qassar and A.-G. M Al-Daher, "Synthesis and characterization of Co (II), Ni (II), Cu (II), and Zn (II) complexes with 2-furaldehyde-2-thenoylhydrazone," *Rafidain J. Sci.*, **2011**, *22*(7), 109–120.
27. D. M. Griffith "Suberoylanilide hydroxamic acid, a potent histone deacetylase inhibitor; its X-ray crystal structure and solid state and solution studies of its Zn(II), Ni(II), Cu(II) and Fe(III) complexes," *J. Inorg. Biochem.*, **2011,** *105*(6), 763–769.
28. L. ZHU.; J. ZHU.; S. FU.; X. GUO, and Y. Wang, "Preparation of molecularly imprinted polymer and its recognition property for salvianolic acid A," *Chem. Res. Appl.*, **2011**.
29. K. Sirivibulkovit.; S. Nouanthavong, and Y. Sameenoi, "based DPPH assay for antioxidant activity analysis," *Anal. Sci.*, **2018,** *34*(7), 795–800.
30. K. Pyrzynska and A. Pλkal, "Application of free radical diphenylpicrylhydrazyl (DPPH) to estimate the antioxidant capacity of food samples," *Anal. Methods.*, **2013**, *5*(17), 4288–4295.

31. W. Al Zoubi.; F. Karabet.; R. Al Bandakji, and K. Hussein, "Experimental and theoretical investigations of the antioxidant activity of 2, 2λmethylenebis (4, 6λdialkylphenol) compounds," *Appl. Organomet. Chem.*, **2017,** *31*(2), e3562.
32. A. A. Boligon, M. M. Machado, and M. L. Athayde, "Technical evaluation of antioxidant activity," *Med. Chem.,* **2014,** *4*(7), 517–522.
33. M. N. Sovilj, "Critical review of supercritical carbon dioxide extraction of selected oil seeds," *Acta Period. Technol.*, **2010**, *41*, 105–120.
34. N. U. A. Mohsin.; M. Irfan, and M. N. Aamir, "In Silico Approaches for Novel Drug Discovery Against Coronavirus by Employing the Hybrid Molecular Technique: A Review," *J. Comput. Biophys. Chem.*, **2021**, *20*(07), 667–674.
35. M. Al-Shakban"Novel xanthate complexes for the size-controlled synthesis of copper sulfide nanorods," *Inorg. Chem.*, **2017**, *56*(15), 9247–9254.
36. A. Otero-Calvis.; B. Ramírez-Serrano, and A. Coello-Velazquez, "Selectivity in the flotation of copper with xanthate over other ions present in wastewater: An experimental and computational study," *J. Mol. Graph. Model.,* **2020**, *98*, 107587.
37. H. A. Mohamad.; K. O. Ali.; T. A. Gerber.;and E. C. Hosten, "Novel palladium (II) complex derived from mixed ligands of dithizone and triphenylphosphine synthesis, characterization, crystal structure, and DFT study," *Bull. Chem. Soc. Ethiop.*, **2022**, *36*(3), 617–626.
38. M. Gaber.; H. El-Ghamry.; F. Atlam, and S. Fathalla, "Synthesis, spectral and theoretical studies of Ni (II), Pd (II) and Pt (II) complexes of 5-mercapto-1, 2, 4-triazole-3-imine-2λ-hydroxynaphyhaline," Spectrochim. Acta Part A Mol. *Biomol. Spectrosc.*, **2015**, *137*, 919–929.
39. X. Huang.; Y. Jia.; S. Wang.; X. Ma.; Z. Cao, and H. Zhong, "Novel sodium O-benzythioethyl xanthate surfactant: synthesis, DFT calculation and adsorption mechanism on chalcopyrite surface," *Langmuir.*, **2019,** *35*(47), 15106–15113.
40. I. Waziri.; O. O. Wahab.; G. A. Mala.; S. O. Oselusi.; S. A. Egieyeh, and H. Nasir, "Zinc (II) complex of (Z)-4-((4-nitrophenyl) amino) pent-3-en-2-one, a potential antimicrobial agent: synthesis, characterization, antimicrobial screening, DFT calculation and docking study," *Bull. Chem. Soc. Ethiop.*, **2023**, *37*(3), 633–651.
41. R. G. Pearson, "Absolute electronegativity and hardness correlated with molecular orbital theory," *Proc. Natl. Acad. Sci.*, **1986**, *83*(22), 8440–8441.
42. S. Andotra.; S. Kumar.; M. Kour.;V. Sharma.; S. Jaglan, and S. K. Pandey, "Synthesis, spectroscopic, DFT and in vitro biological studies of vanadium(III) complexes of aryldithiocarbonates," Spectrochim. Acta Part A Mol. *Biomol. Spectrosc.*, **2017**, *180*, 127–137.
43. X. Ma.; L. Xia.; S. Wang.; H. Zhong, and H. Jia, "Structural modification of xanthate collectors to enhance the flotation selectivity of chalcopyrite," *Ind. Eng. Chem. Res.*, **2017,** *56*(21), 6307–6316.
44. R. G. Parr.; L. v Szentpály, and S. Liu, "Electrophilicity index," *J. Am. Chem. Soc.*, **1999**, *121*(9), 1922–1924.
45. X. Yang.; B. Albijanic.; G. Liu, and Y. Zhou, "Structure–activity relationship of xanthates with different hydrophobic groups in the flotation of pyrite," *Miner. Eng.*, **2018**, *125*, 155–164.
46. M. M. Milosavljevi "New eco-friendly xanthate-based flotation agents," *Minerals.*, **2020**, *10*(4), 350.